Protein Science (1999), *8*:1904–1907. Cambridge University Press. Printed in the USA.

FOR THE RECORD

Monomer-trimer equilibrium of the ectodomain of SIV gp41: Insight into the mechanism of peptide inhibition of HIV infection

MICHAEL CAFFREY,[1] JOSHUA KAUFMAN,[2] STEPHEN STAHL,[2] PAUL WINGFIELD,[2] ANGELA M. GRONENBORN,[1] AND G. MARIUS CLORE[1]

[1]Laboratory of Chemical Physics, Building 5, National Institute of Diabetes and Digestive and Kidney Diseases, National Institutes of Health, Bethesda, Maryland 20892-0520
[2]Protein Expression Laboratory, Building 6B, National Institute of Arthritis and Musculoskeletal Diseases, National Institutes of Health, Bethesda, Maryland 20892

(RECEIVED March 29, 1999; ACCEPTED May 11, 1999)

Abstract: The monomer-trimer equilibrium of the ectodomain of SIV gp41 (residues 27–149, e-gp41) has been characterized by analytical ultracentrifugation, circular dichroism (CD), and NMR spectroscopy. Based on analytical ultracentrifugation experiments performed at different rotor speeds and protein concentrations, the equilibrium association constant for the SIV e-gp41 trimer is 3.1×10^{11} M^{-2}. The presence of intermolecular nuclear Overhauser effects in a mixture of ^{12}C and ^{13}C-labeled e-gp41 prepared under nondenaturing conditions unambiguously demonstrates that there is a dynamic equilibrium between the monomer and trimer. The CD spectra taken as a function of SIV e-gp41 concentration suggest that the helical content of the monomeric state does not change significantly relative to that of the trimeric state. The relevance of the monomer-trimer equilibrium is discussed with respect to gp41 function and the inhibitory properties of gp41 peptides.

Keywords: gp41; monomer; trimer; HIV; SIV; peptide inhibition

gp41 mediates the fusion event in HIV and SIV infection (Frankel & Young, 1998). We have previously characterized the solution and dynamic properties of the ectodomain of SIV gp41 (e-gp41), which is a soluble domain consisting of residues 27–149 (Caffrey et al., 1997, 1998a, 1998b; Wingfield et al., 1997). The solution structure of SIV e-gp41 (Caffrey et al., 1998a), as well as the crystal structures of peptide fragments of HIV and SIV e-gp41 (Chan et al., 1997; Tan et al., 1997; Weissenhorn et al., 1997; Malashkevich et al., 1998), clearly demonstrate that e-gp41 exists as a stable symmetric trimer with a $T_m = 100\,^{\circ}C$ (Caffrey et al., 1998a). It has been shown, however, by analytical ultracentrifugation that significant amounts of monomer may be present at physiological concentrations (Wingfield et al., 1997). Indeed, the presence of the monomer has been suggested as a novel explanation for the inhibitory properties of gp41 peptides (Caffrey et al., 1998a). In this paper we further characterize the monomer-trimer equilibrium of SIV e-gp41 by analytical ultracentrifugation, CD, and NMR spectroscopy.

Previously, we reported that analytical ultracentrifugation experiments suggested that the molecular weights of the SIV and HIV e-gp41 were less than expected for stable trimers. The equilibrium data were best modeled as a reversible monomer-trimer system that obtained approximate estimates for the equilibrium association constants (Wingfield et al., 1997). We extend our previous work to investigate the effects of rotor speed and protein concentration on the molecular association of SIV e-gp41. A typical result is shown in Figure 1A; the data presented were derived from a global fit of SIV e-gp41 analyzed at three rotor speeds (see Methods). The derived equilibrium association constant (K_a) of 3.1×10^{11} M^{-2} is relatively close to that previously reported (1.5×10^{11} M^{-2}); however, the latter analysis was performed at only a single rotor speed (16,000 RPM) (Wingfield et al., 1997). Since both SIV and HIV e-gp41 have rod-like helical structures (Weissenhorn et al., 1996, 1997; Chan et al., 1997; Tan et al., 1997; Caffrey et al., 1998a; Malashkevich et al., 1998), an obvious concern in interpreting the sedimentation equilibrium data arises from the effects of nonideality (McRorie & Voelker, 1993). These effects are difficult to measure but can be minimized by sample dilution and increasing the ionic strength of the solvent. In the case of SIV e-gp41, the inclusion of 50–100 mM NaCl or dilution of the sample starting concentration (from 0.37 to 0.09 mg/mL) had no significant effect on the calculated equilibrium association constant.

Reprint requests to: G. Marius Clore, Laboratory of Chemical Physics, Building 5, National Institute of Diabetes and Digestive and Kidney Diseases, National Institutes of Health, Bethesda, Maryland 20892-0520; e-mail: clore@speck.niddk.nih.gov.

Abbreviations: CD, circular dichroism; e-gp41, ectodomain of gp41; Gdn-HCl, guanidine hydrochloride; HIV, human immunodeficiency virus; NMR, nuclear magnetic resonance; NOE, nuclear Overhauser effect; SIV, simian immunodeficiency virus.

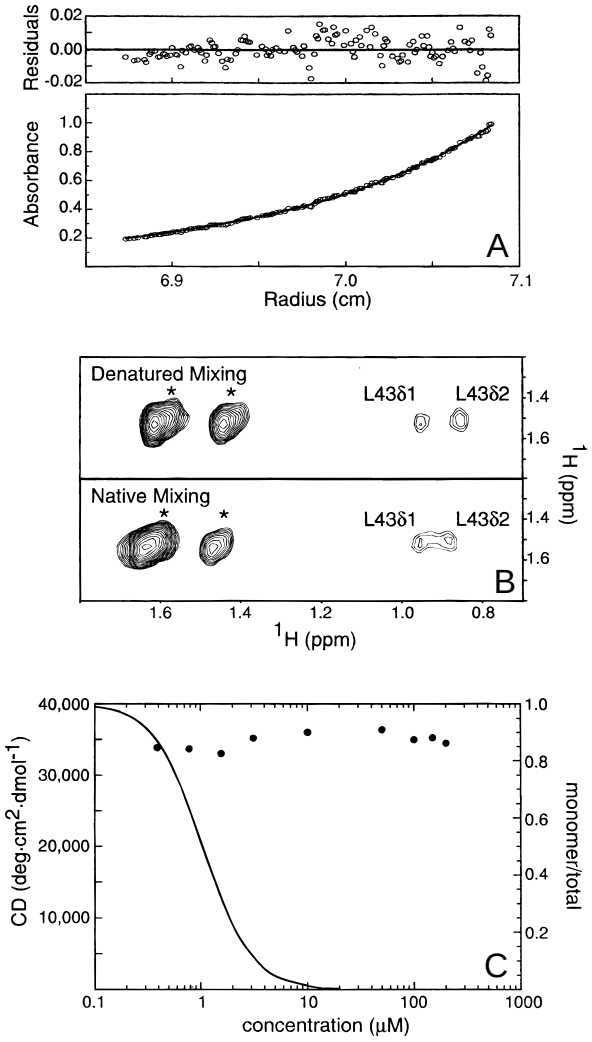

Fig. 1. Characterization of the monomer-trimer equilibrium of SIV e-gp41 by analytical ultracentrifugation, NMR and CD. **A:** The absorbance gradient (determined at 280 nm) in the centrifuge cell after attaining sedimentation equilibrium of SIV e-gp41 is shown in the bottom panel. The solid line is the result of fitting to a monomer-trimer system, and the open circles are the experimental values. The data correspond to a global fit for three independent experiments performed at 12,000, 16,000, and 20,000 rpm. A starting protein concentration of 0.18 mg/mL was used in each case. The corresponding top panel shows the difference in the fitted and experimental values as a function of radial position (residuals). **B:** Two-dimensional plane from the three-dimensional ^{13}C-separated/^{12}C-filtered three-dimensional NOE experiment (80 ms mixing time) illustrating intermolecular NOEs from the methyl group of Ala133 to the δ1 and δ2 methyl groups of Leu143. The sample in the top panel was prepared by mixing equimolar amounts of denatured ^{12}C/^{14}N and ^{13}C/^{15}N labeled SIV e-gp41, while that in the bottom panel was prepared by mixing equimolar amounts of native ^{12}C/^{14}N and ^{13}C/^{15}N labeled SIV e-gp41. Autocorrelations corresponding to the residual diagonal peaks are denoted by asterisks. Note that the chemical shifts of the δ1 and δ2 methyl protons of Leu43 are slightly shifted in the two spectra due to small differences in pH. **C:** 220 nm CD signal as a function of SIV e-gp41 protein concentration. The ratio of monomer to total protein concentration, calculated for a monomer-trimer equilibrium with a K_a of 3.1×10^{11} M^{-2}, is plotted as a solid line.

The analytical ultracentrifugation studies indicate that SIV and HIV e-gp41 exist as an equilibrium between the monomeric and trimeric states. NMR studies are typically performed at millimolar protein concentrations where the e-gp41 monomer would be expected to be present at less than 1% and was thus not observed in our NMR studies (Caffrey et al., 1997, 1998a). A ^{12}C/^{14}N:^{13}C/^{15}N mixed sample was prepared under nondenaturing conditions (10 mM sodium acetate, pH 3.0) at a protein concentration nearer the K_d (1 μM protein concentration) to favor the presence of the monomeric species and thus facilitate mixing of the ^{12}C/^{14}N and ^{13}C/^{15}N species to form a heterotrimer. In contrast, the original ^{12}C/^{14}N:^{13}C/^{15}N mixed sample of e-gp41 was prepared under partially denaturing conditions in 6 M guanidine hydrochloride (Gdn-HCl). An example of a two-dimensional plane from a three-dimensional ^{12}C-filtered/^{13}C-separated NOE spectrum is shown in Figure 1B (top panel) from a sample prepared under denaturing conditions (6 M Gdn-HCl). Note the presence of long-range intermolecular (i.e., intersubunit) NOEs between the methyl group of Ala133 and the methyl groups of Leu43. In Figure 1B (bottom panel) the presence of the same intermolecular NOEs in a sample prepared under nondenaturing conditions unambiguously demonstrates that the monomer-trimer equilibrium exists.

To characterize the structure of the e-gp41 monomeric state, CD spectra were taken as a function of protein concentration (Fig. 1C). For protein concentrations from 0.38–200 μM, no change in the mean residue ellipticity at 220 nm, which is characteristic of helices, is apparent. Based on the K_a, the monomer concentration is expected to be greater than the trimer concentration for protein concentrations less than 3 μM. The absence of change in the CD signal at lower protein concentrations indicates that the monomer secondary structure is not significantly different from that of an individual subunit in the trimer. The observation that peptides corresponding to the C-terminal helix are unstructured in isolation (Blacklow et al., 1995; Lu et al., 1995) suggests that the tertiary structure of the monomer does not change significantly between the monomeric and trimeric states.

Peptides corresponding to the N- or C-terminal helices inhibit HIV infection (Wild et al., 1992, 1994). Indeed, a peptide corresponding to part of the C-terminal helix (T20) is currently undergoing stage II clinical trials as a new anti-HIV drug (Kilby et al., 1998). Consequently, it is of interest to understand the molecular basis for peptide inhibition of HIV infection. Based on the premise of the monomer-trimer equilibrium, we have presented a model to account for the observed peptide inhibition of HIV infection (Caffrey et al., 1998a). The present sedimentation equilibrium and NMR data more clearly establish the existence of the monomeric state, and the CD data suggest that the monomeric state remains largely helical. The equilibrium between the monomeric and trimeric states, as well as the gp41-inhibitory peptide, are modeled in Figure 2. In this model, the inhibitory C-terminal peptides can bind to either the monomeric or trimeric states (M or T). Accordingly, the M-P and T-P states would not be competent for gp41-mediated fusion. Based on the e-gp41 solution structure, the surface area of the contact region between the C-terminal helix and the neighboring N-terminal helices would be expected to be reduced from 1,679–925 Å^2 upon monomerization (Caffrey et al., 1998a). Thus, we suggest that binding of the C-terminal peptide to state M is most favored due to the reduced interaction between the N- and C-terminal helices. Moreover, the inhibitory N-terminal peptides, which are less potent inhibitors (presumably due to self-association) than the C-terminal peptides (Lu et al., 1995), would also most likely bind to the monomeric state. Finally, it is important to note that there are a number of differences between the ectodomain analyzed here and the ectodomain that exists in vivo. These dif-

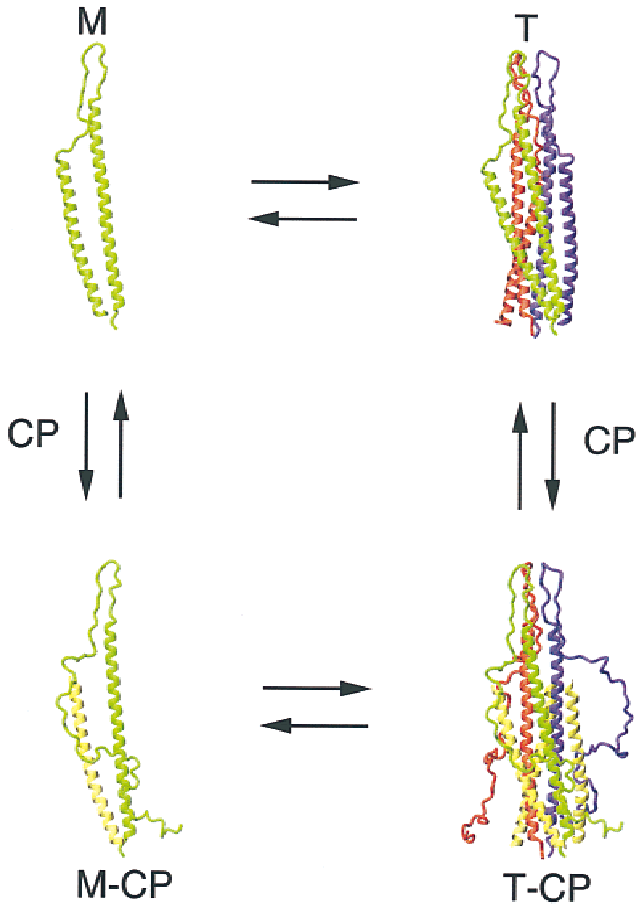

Fig. 2. Model for the monomer-trimer equilibrium of gp41 and the proposed effects of inhibitory peptides. There are four states: monomer (M), timer (T), monomer-C peptide (M-CP), and trimer-C peptide (T-CP). The subunits of gp41 are colored red, green, and blue; the inhibitory C peptides (residues 106–149) are colored yellow.

ferences include: (1) tethering of the ectodomain to the membrane in vivo, (2) the presence of glycosyl groups in native gp41, and (3) the binding of gp120 to gp41 during the initial stages of HIV infection. All of these differences are likely to affect the monomer-trimer equilibrium. Nonetheless, the monomer-trimer equilibrium clearly observed in vitro may well reflect the monomer-trimer equilibrium in vivo.

Methods: Protein samples were prepared as described (Wingfield et al., 1997). Analytical ultracentrifugation experiments were performed at 20 °C using a Beckman Optima XL-1 analytical ultracentrifuge with an An-60 Ti rotor and standard double sector cells. Samples were independently rotated at 12,000, 16,000, and 20,000 rpm for 15–18 h. After collecting the sedimentation equilibrium data, the rotor was accelerated to 45,000 rpm for 3–4 h to determine baseline corrections. Protein samples in 50 mM sodium formate, pH 3.1, had starting concentrations of between 0.09–0.37 mg/mL. A partial specific volume of 0.737 m^{-1} L^3 was used. Association constants for the monomer-trimer self-association model derived from the ultracentrifuge data were converted to molar units using the following equation: $K_{abs}\epsilon^2\lambda^2/3 = K_a$ (M^{-2}) where $K_{abs} = K_{1-3}$ in absorbency units, ϵ is the molar extinction coefficient (3.68×10^4 M^{-1} cm^{-1}), and λ is the pathlength of the centrifugation cell (1.2 cm). The original mixed NMR sample was prepared by mixing equimolar amounts of $^{12}C/^{14}N$ and $^{13}C/^{15}N$-labeled protein in 6 M Gdn-HCl and 50 mM Tris-HCl, pH 8.0, and refolding as described (Caffrey et al., 1997, 1998a). The present mixed NMR sample was prepared by mixing equimolar amounts of $^{12}C/^{14}N$ and $^{13}C/^{15}N$-labeled protein and diluting to ~1 μM protein concentration in 10 mM acetate, pH 3.0, and stirring overnight at room temperature. Subsequently, the mixed samples were concentrated by ultrafiltration using an Amicon centricon-30 at 15 °C. The final solution conditions for the NMR experiments were ~2 mM (in monomer) e-gp41 in 50 mM deuterated sodium formate, pH 3.0. The three-dimensional ^{12}C-filtered/^{13}C-separated NOE experiments (Clore & Gronenborn, 1998) with a mixing time of 80 ms were recorded on a Bruker DMX 750 equipped with a triple resonance *x,y,z* gradient shielded probe operating at 45 °C. The conditions for the CD experiments, recorded on a Jasco J-720 spectropolarimeter with 0.1–10 mm cell path lengths, were 50 mM sodium formate, pH 3.0 at 25 °C.

Acknowledgments: This work was supported by the AIDS Targeted Antiviral Program of the Office of the Director of the National Institutes of Health (to G.M.C., A.M.G, and the Protein Expression Laboratory).

References

Blacklow S, Lu M, Kim P. 1995. A trimeric subdomain of the simian immunodeficiency virus envelope glycoprotein. *Biochemistry 34*:14955–14962.

Caffrey M, Cai M, Kaufman J, Stahl SJ, Wingfield PT, Gronenborn AM, Clore GM. 1997. Determination of the secondary structure and global topology of the 44 kDa ectodomain of gp41 of the simian immunodeficiency virus by multidimensional nuclear magnetic resonance spectroscopy. *J Mol Biol 271*:819–826.

Caffrey M, Cai M, Kaufman J, Stahl S, Wingfield P, Covell D, Gronenborn AM, Clore GM. 1998a. Three-dimensional solution structure of the 44 kDa ectodomain of SIV gp41. *EMBO J 17*:4572–4584.

Caffrey M, Kaufman J, Stahl S, Wingfield P, Gronenborn AM, Clore GM. 1998b. 3D NMR experiments for measuring ^{15}N relaxation data in large proteins: Application to the 44 kDa ectodomain of SIV gp41. *J Magn Reson 135*:368–372.

Chan DC, Fass D, Berger JM, Kim PS. 1997. Core structure of gp41 from the HIV envelope glycoprotein. *Cell 89*:263–273.

Clore GM, Gronenborn AM. 1998. Determining the structures of large proteins and protein complexes by NMR. *Trends Biotech 16*:22–34.

Frankel AD, Young JA. 1998. HIV-1: Fifteen proteins and an RNA. *Ann Rev Biochem 67*:1–25.

Kilby JM, Hopkins S, Venetta TM, DiMassimo B, Cloud GA, Lee JY, Alldredge L, Hunter E, Lambert D, Bolognesi D. 1998. Potent suppression of HIV-1 replication in humans by T-20, a peptide inhibitor of gp41-mediated virus entry. *Nat Medicine 4*:1302–1307.

Lu M, Blacklow S, Kim P. 1995. A trimeric structural domain of the HIV-1 transmembrane glycoprotein. *Nature Struct Biol 2*:1075–1082.

Malashkevich VN, Chan DC, Chutowski CT, Kim PS. 1998. Crystal structure of the simian immunodeficiency virus (SIV) gp41 core: Conserved helical interactions underlie the broad inhibitory activity of gp41 peptides. *Proc Natl Acad Sci USA 95*:9134–9139.

McRorie DK, Voelker PJ. 1993. Publication 362784 Beckman Instruments Inc., Fullerton, California.

Tan K, Liu JH, Wang JH, Shen S, Lu M. 1997. Atomic structure of a thermostable subdomain of HIV-1 gp41. *Proc Natl Acad Sci USA 94*:12203–12308.

Weissenhorn W, Dessen A, Harrison SC, Skehel JJ, Wiley DC. 1997. Atomic structure of the ectodomain from HIV-1 gp41. *Nature (London) 387*:426–430.

Weissenhorn W, Wharton S, Calder L, Earl P, Moss B, Aliprandis E, Skehel JJ, Wiley D. 1996. The ectodomain of HIV-1 envelope subunit gp41 forms a

soluble, α-helical, rod-like oligomer in the absence of gp120 and the N-terminal fusion peptide. *EMBO 15*:1507–1514.

Wild CT, Oas T, McDanal CB, Bolognesi D, Matthews TJ. 1992. A synthetic peptide inhibitor of human immunodeficiency virus replication: Correlation between solution structure and viral inhibition. *Proc Natl Acad Sci USA 89*:10537–10541.

Wild CT, Shugars DC, Greenwell TK, McDanal CB, Matthews TJ. 1994. Peptides corresponding to a predictive α-helical domain of human immunodeficiency virus type 1 gp41 are potent inhibitors of virus infection. *Proc Natl Acad Sci USA 91*:9770–9774.

Wingfield PT, Stahl SJ, Kaufman J, Zlotnick A, Hyde CC, Gronenborn AM, Clore GM. 1997. The extracellular domain of immunodeficiency virus gp41 protein. Expression in *Escherichia coli*, purification, and crystallization. *Protein Sci 6*:1653–1660.